

**Electronic Supplementary Information (ESI)**

**A bimodal MRI and NIR liposome nanoprobe for tumor targeted molecular imaging**

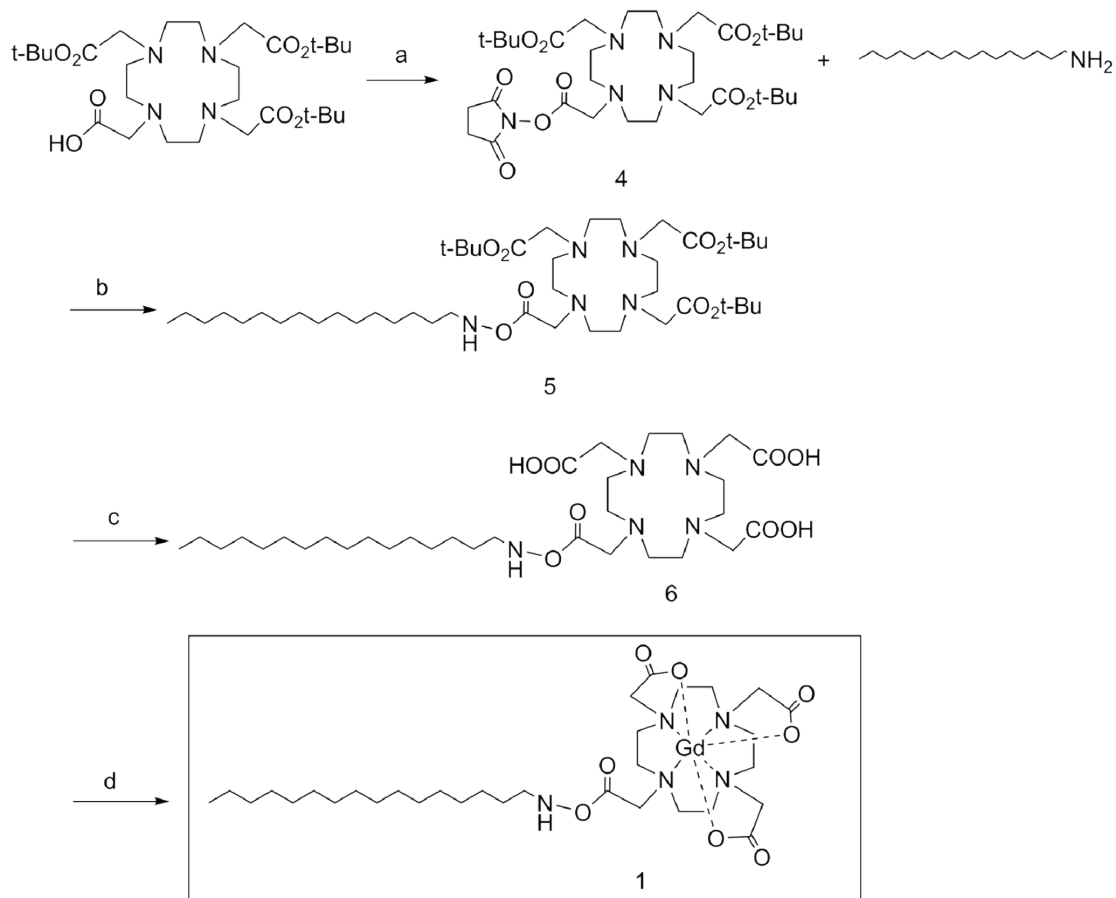
Huihui Wang<sup>a,b</sup>, Hao Wu<sup>a,b</sup>, Hujun Shen<sup>d</sup>, Shaote Geng<sup>c</sup>, Beibei, Wang<sup>a,b</sup>, Yanfang Wang<sup>a,b</sup>, Xiaojun Ma<sup>a</sup>, Guohui Li<sup>d</sup> and Mingqian Tan<sup>a,c,\*</sup>

<sup>a</sup>*Division of Biotechnology, Dalian Institute of Chemical Physics, Chinese Academy of Science, Dalian 116023, China. Fax & Tel: +86-411-84379139; E-mail: 2468750030@qq.com.*

<sup>b</sup>*University of the Chinese Academy of Science, Beijing 100049, China.*

<sup>c</sup>*National Engineering Research Center of Seafood, Liaoning Province Key Laboratory of Seafood Science and Technology, School of Food Science and Technology, Dalian Polytechnic University, Dalian 116034, China.*

<sup>d</sup>*Molecular Modeling and Design Group, State Key Laboratory of Molecular Reaction Dynamics, Dalian Institute of Chemical Physics, Chinese Academy of Science, Dalian 116023, China.*



Scheme S1. a) DCC, NHS,  $\text{CH}_2\text{Cl}_2$ , 2 h; b)  $\text{Et}_3\text{N}$ ,  $\text{CH}_2\text{Cl}_2$ , 12 h; c)  $\text{TFA}-\text{CH}_2\text{Cl}_2$  1:1 v/v, 2 h; d)  $\text{Gd}(\text{CH}_3\text{COO})_3 \cdot \text{H}_2\text{O}$ , 90 °C, 12 h.

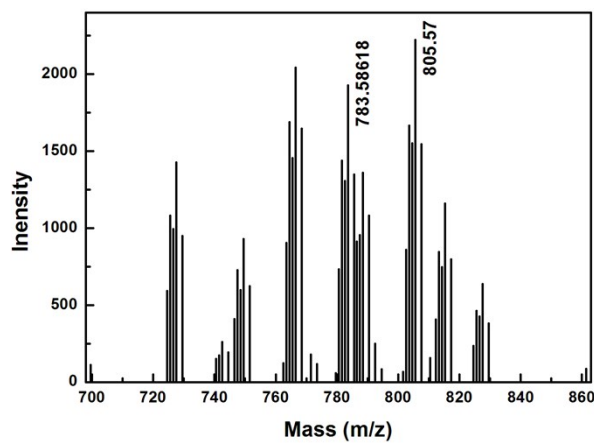


Fig. S1. MALDI-TOF mass spectrum of Gd-DOTA-HDA.

### Xylenol orange test

The sample of Gd-DOTA-HDA was dialysed (molecule weight cutoff 500 Da)

against PBS for 7 days. The outer PBS solution (dialyzate) was subjected to the Xylenol orange test. The leak and presence of free  $\text{Gd}^{3+}$  ions in the Gd-incorporated compounds was determined by measuring the absorbance at 573 nm of a mixture of Xylenol orange solution (0.5 mM) in 990  $\mu\text{L}$  sodium acetate buffer (0.1 M, pH 5.2) and test solution (Gd compound in 10  $\mu\text{L}$  water).<sup>1</sup>

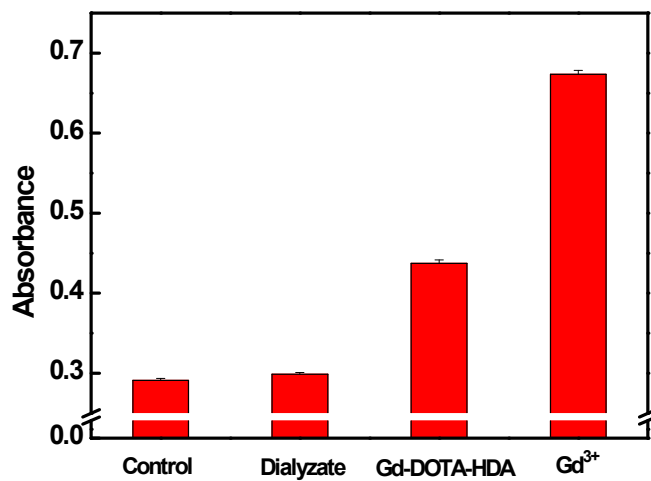
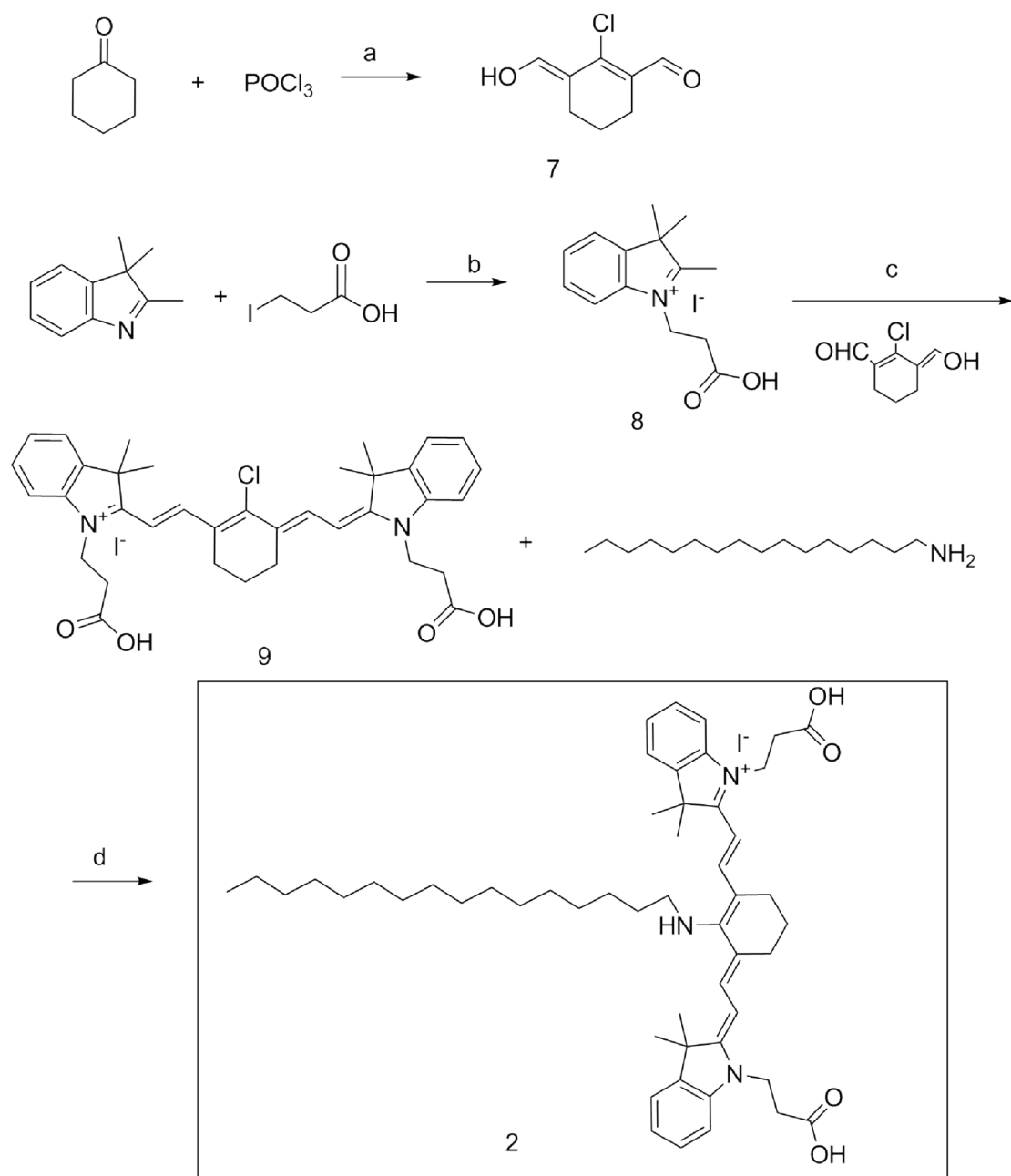


Fig. S2  $\text{Gd}^{3+}$  leaking and stability experiment of Gd-DOTA-HDA by a Xylenol orange test. PBS solution was used for control experiment. Dialyzate was the outer PBS solution after 7 days dialysis. Gd-DOTA-HDA was put into the dialysis bag with molecule weight cutoff 500 Da against PBS for 7 days. The free  $\text{Gd}^{3+}$  concentration in PBS was 5mM.



Scheme S2. a) DMF, DCM,  $\text{N}_2$ , 80 °C, 3 h, 33%; b) toluene, 100 °C,  $\text{N}_2$ , 3 h, 65%; c) DMF, toluene,  $\text{N}_2$ , 160 °C, 10 h, 31% ; d)  $\text{Et}_3\text{N}$ , DMF,  $\text{N}_2$ , 70 °C, 10 h, 23%.

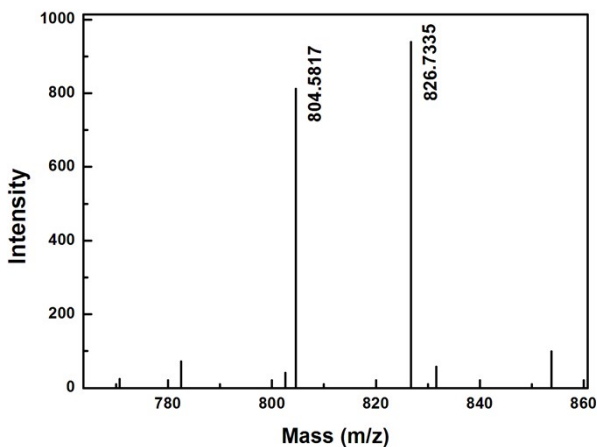
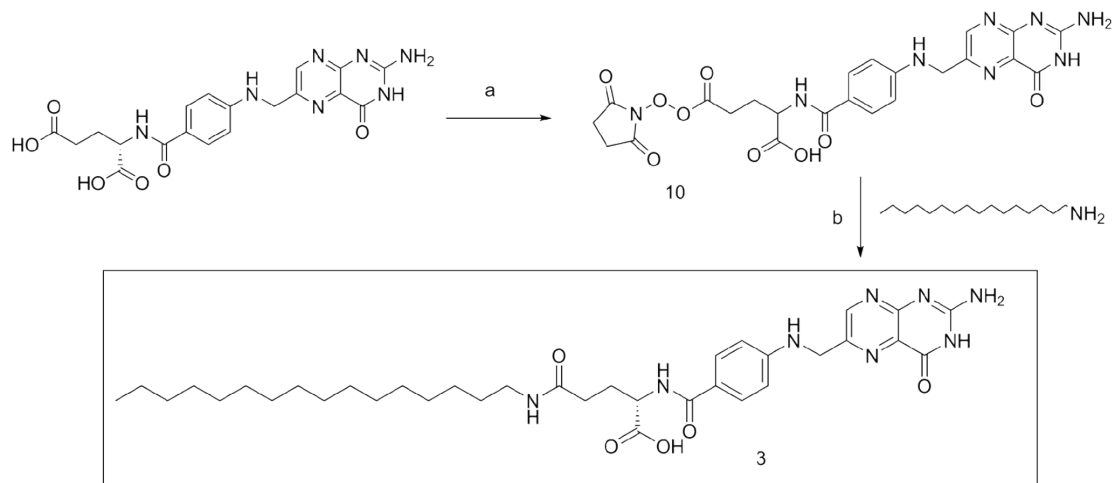


Fig. S3. MALDI-TOF mass spectrum of Cy7-HDA.



Scheme S3. a)  $\text{Et}_3\text{N}$ , DCC, NHS, DMSO, 12 h; b)  $\text{Et}_3\text{N}$ , DMSO-ethyl acetate 3:2 v/v, 24 h, 37%.

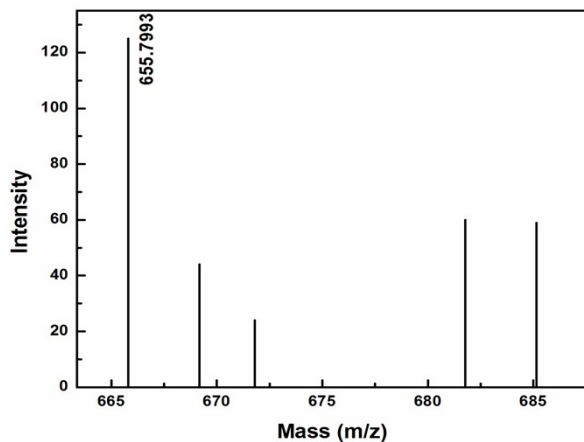


Fig. S4. MALDI-TOF mass spectrum of FA-HDA.

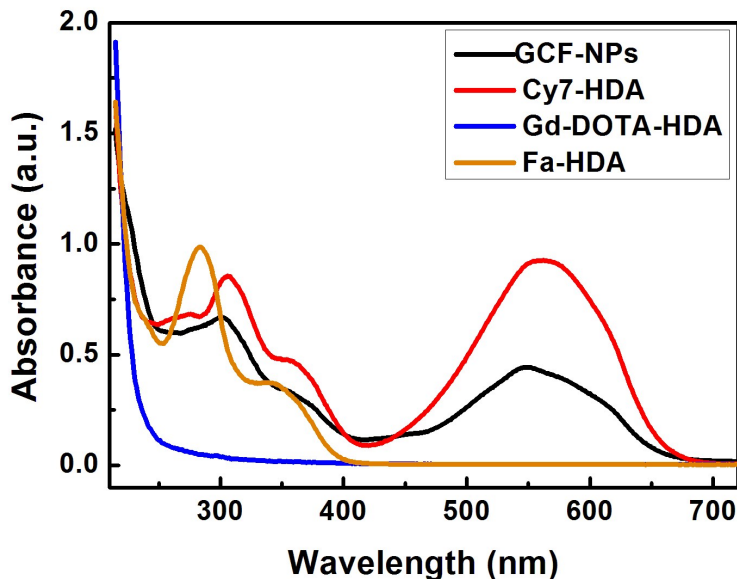


Fig. S5. Absorption spectra of GCF-HDA NPs, Cy7-HDA, Gd-DOTA-HDA, FA-HDA in water. GCF-HDA NPs: Gd-DOTA-HDA, Cy7-HDA and FA-HDA nanoparticles.

With increasing computational power for molecular modeling, it has become popular to use molecular dynamics (MD) simulation to model biomaterials because it provides an insightful understanding of the functions of biomaterials at a molecular level<sup>2,3</sup>. However, due to large degrees of freedom and a small integration step, the accessibility of a traditional MD simulation is limited to some biological processes occurring at the timescales faster than microsecond. To enhance the capability of a MD simulation, a simplified model, namely Coarse-Grained (CG) model, is a good choice as the atomistic resolution of a biomolecular system is properly reduced<sup>4-6</sup>. To develop an effective CG model, it is critical to acquire an effective potential describing accurately the interactions between coarse-grained particles. Gay-Berne potential<sup>7-9</sup>, which is a well-known anisotropic potential, has been wildly used for

describing the CG particles being considered to be elliptic. ACG model, adopting the framework by combining Gay-Berne with point electric multipole (EMP) potentials, has successfully been applied to model liquid waters, organic liquids and proteins.<sup>10-12</sup>

### **GBEMP mapping for self-assembly units**

GBEMP mapping for three self-assembly units is depicted in Figure S6. The CG model of Cy7-HDA (C) is composed of one elliptic rigid body and three disk-like rigid bodies, that of Gd-DOTA-HDA (D) is made up of four elliptic rigid bodies and that of FA-HDA (F) consists of one elliptic rigid body and one disk-like rigid body. The hydrophobic tail of each model is represented by one elliptic rigid body that contains one Gay-Berne site and one non-interacting EMP site. The non-interacting EMP site (denoted by orange filled circle) would not involve in electrostatic interaction but serve just as the connection purpose. In each model, the corresponding CG particles of hydrophilic head group contain one Gay-Berne site and one EMP site which both share a same location shown by a red filled circle. In addition, one or two non-interacting EMP sites are included into each CG particle in order to connect two different rigid bodies.

### **GBEMP energy function**

The effective energy function of GBEMP model is given by a sum of bonded and non-bonded energy terms:

$$U_{GBEMP} = U_{bond} + U_{angle} + U_{torsion} + U_{GB} + U_{EMP} \quad (1)$$

where  $U_{bond}$ ,  $U_{angle}$  and  $U_{torsion}$  represent the bond stretching, angle bending and torsional potentials respectively. The non-bonded energy terms are described by  $U_{GB}$

and  $U_{EMP}$  that correspond to Gay-Berne anisotropic potential and electric multipole potential respectively.

In the GBEMP model, a fourth-order Taylor expansion of the Morse potential is used for the bond stretching energy term when the angle bending energy term adopts a sixth-order potential, and a three-term Fourier series expansion is employed to calculate torsional energies:

$$U_{bond} = K_b(b - b_0)^2 \left[ 1 - 2.55(b - b_0) + \left( \frac{7}{12} \right) 2.55(b - b_0)^2 \right] \quad (2)$$

$$\begin{aligned} U_{angle} = K_\theta(\theta - \theta_0)^2 & [1 - 0.014(\theta - \theta_0) + 5.6 \times 10^{-5}(\theta - \theta_0)^2 \\ & - 7.0 \times 10^{-7}(\theta - \theta_0)^3 + 2.2 \times 10^{-8}(\theta - \theta_0)^4] \end{aligned} \quad (3)$$

$$U_{torsion} = \sum_n K_{n\phi} [1 + \cos(n\phi \pm \delta)] \quad (4)$$

In this work, the bond stretching, angle bending and torsional potentials were parametrized by fitting to the atomistic profiles of the potentials of mean force (PMFs) constructed from atomistic conformations of self-assembly units (Figure S7).

The Gay-Berne anisotropic potential energy function  $U_{GB}$  is given as the form:

$$\begin{aligned} U_{GB}(\hat{u}_i \hat{u}_j \hat{r}_{ij}) &= 4\varepsilon(\hat{u}_i \hat{u}_j \hat{r}_{ij}) \left[ \left( \frac{d_w \sigma_0}{r_{ij} - \sigma(\hat{u}_i \hat{u}_j \hat{r}_{ij}) + d_w \sigma_0} \right)^{12} - \left( \frac{d_w \sigma_0}{r_{ij} - \sigma(\hat{u}_i \hat{u}_j \hat{r}_{ij}) + d_w \sigma_0} \right)^6 \right] \end{aligned} \quad (5)$$

The range parameter  $\sigma(\hat{u}_i \hat{u}_j \hat{r}_{ij})$  and the strength parameter  $\varepsilon(\hat{u}_i \hat{u}_j \hat{r}_{ij})$  for pair-wise interactions are functions of the relative orientation of the Gay-Berne particles  $i$  and  $j$ . Each uniaxial molecule is associated with a set of Gay-Berne parameters that describe its shape (such as ellipsoid, sphere or disk) and the orientation of its principal axis in

the inertial frame, defined according to its all-atom model. The term  $d_w$  is used to control the “softness” of the potential and  $\sigma_0$  is defined as the square root of the sum of squared breadth of each particle. To parametrize the Gay-Berne potentials for nucleic acid models (shown in Figure S6), the atomistic energy profiles (using OPLS atomistic force field in this study) were constructed for the intermolecular van der Waals (VDW) interactions between two identical molecular fragments (homodimer), illustrated in Figure S8. In each case, diverse configurations were generated with different orientations (such as, cross, end-to-end, face-to-face, etc.) as well as at various separations. The initial Gay-Berne parameters for CG particles were derived through fitting to the corresponding atomistic energy profiles in gas phase using a generic algorithm.

The interaction energy between two electric multipole sites can be expressed as its polytensor form:

$$U_{EMP} = \sum_{ij} U_{ij} = \sum_{ij} V_i^T M_{ij} V_j \quad (6)$$

or its expanded form

$$U_{ij} = \begin{bmatrix} q_i \\ d_{ix} \\ d_{iy} \\ d_{iz} \\ Q_{ixx} \\ \vdots \end{bmatrix}^T \begin{bmatrix} 1 & \frac{\partial}{\partial x_j} & \frac{\partial}{\partial y_j} & \cdots \\ \frac{\partial}{\partial x_i} & \frac{\partial^2}{\partial x_i \partial x_j} & \frac{\partial^2}{\partial x_i \partial y_j} & \cdots \\ \frac{\partial}{\partial y_i} & \frac{\partial^2}{\partial y_i \partial x_j} & \frac{\partial^2}{\partial y_i \partial y_j} & \cdots \\ \vdots & \vdots & \ddots & \ddots \end{bmatrix} \begin{pmatrix} q_j \\ d_{jx} \\ d_{jy} \\ d_{jz} \\ Q_{jxx} \\ \vdots \end{pmatrix} \quad (7)$$

Where  $q$ ,  $d$  and  $Q$  are charge, dipole and quadrupole moment, respectively. When the EMP sites are determined in a rigid body, it should be straightforward to obtain the EMP parameters for the CG particle through the electric multipole expansion at the

specific locations based on an atomistic model.

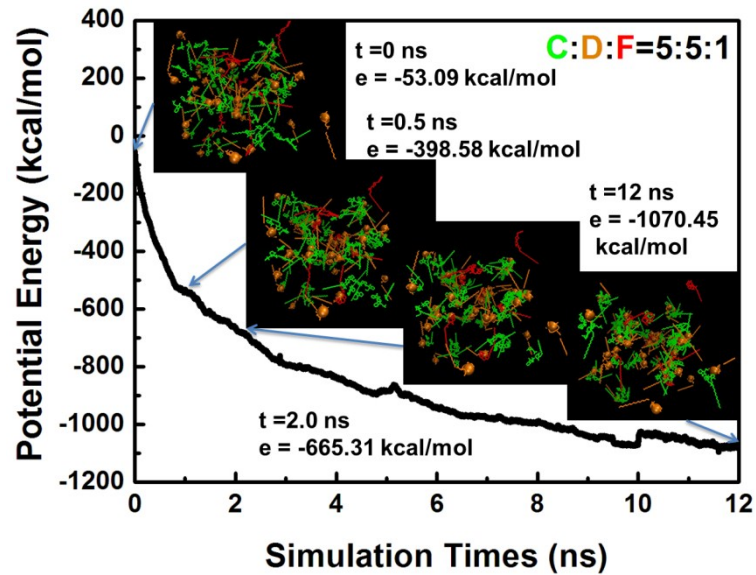


**Figure S6.** Potential energies of the system (the mixture of C, D and F was built in a ratio of 5:5:1) evolving with MD simulation time. The starting structure ( $t = 0$  ns) of the system was constructed as a random form.

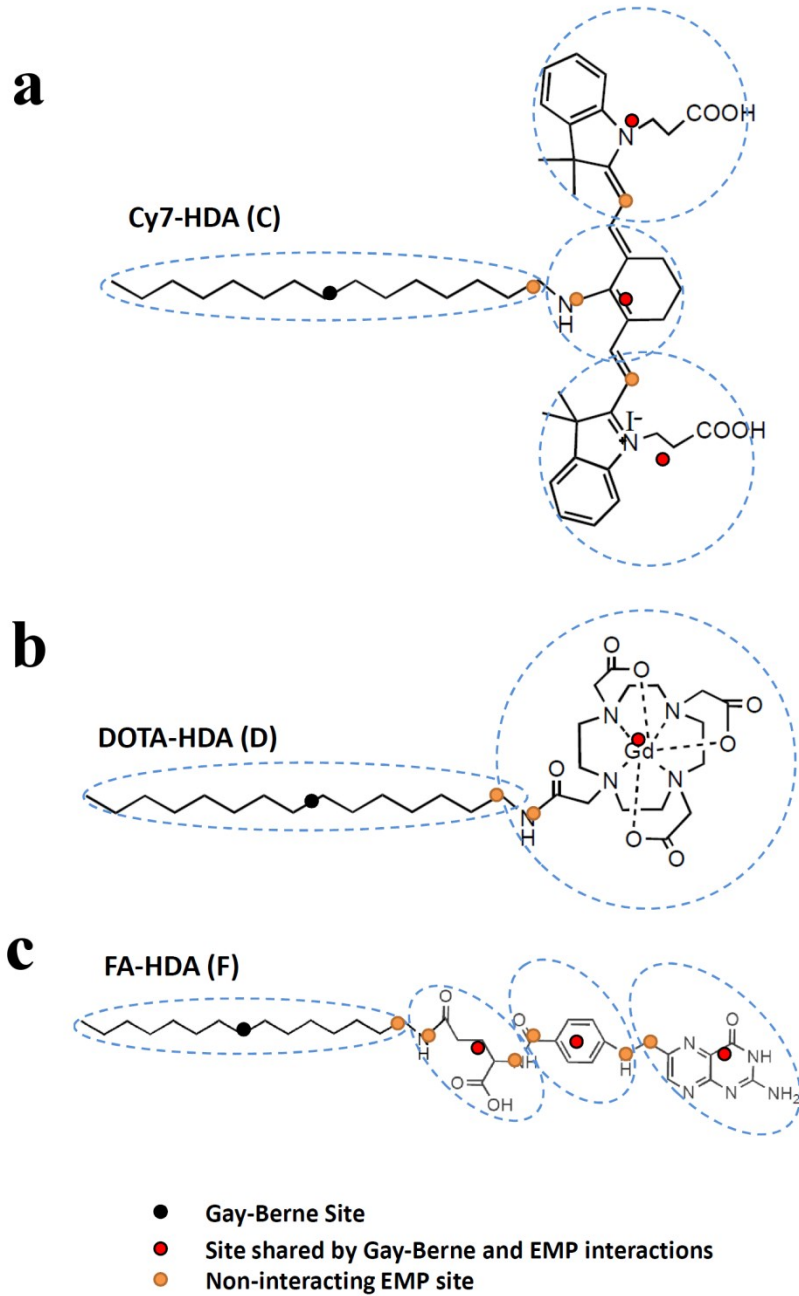


**Figure S7.** GBEMP mapping for (a) Cy7-HDA, (b) Gd-DOTA-HDA and (c) FA-HDA. Each rigid body, being enclosed by a dash line, is composed of a Gay-Berne interacting site and one or more electric multipole (EMP) sites. Gay-Berne interacting sites are indicated black filled circles while the interacting EMP sites and non-interaction EMP sites are indicated by red and orange filled circles respectively. Red filled circles represent the sites shared by Gay-Berne and EMP interactions.

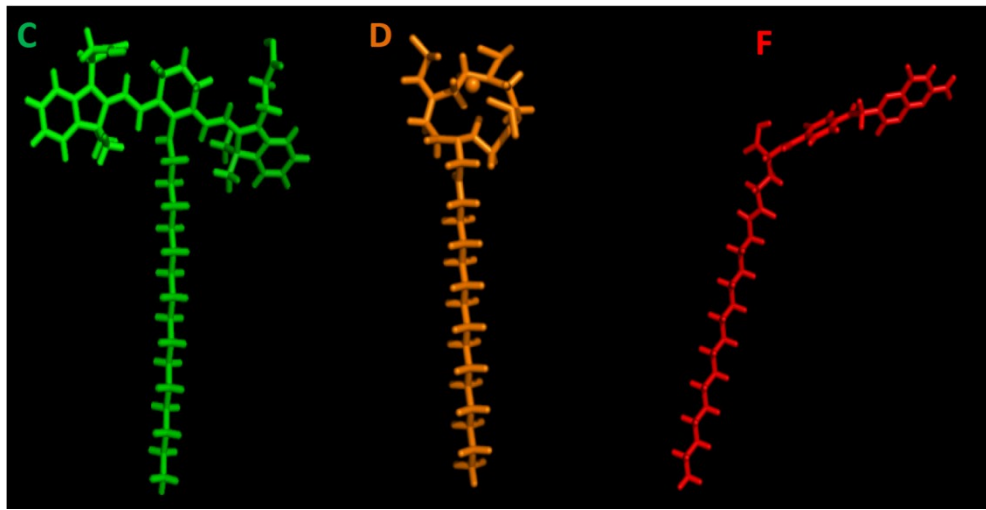


**Figure S8.** Atomistic representation for Cy7-HDA (C), Gd-DOTA-HDA (D) and FA-HDA (F) are in green, orange and red colors, respectively.

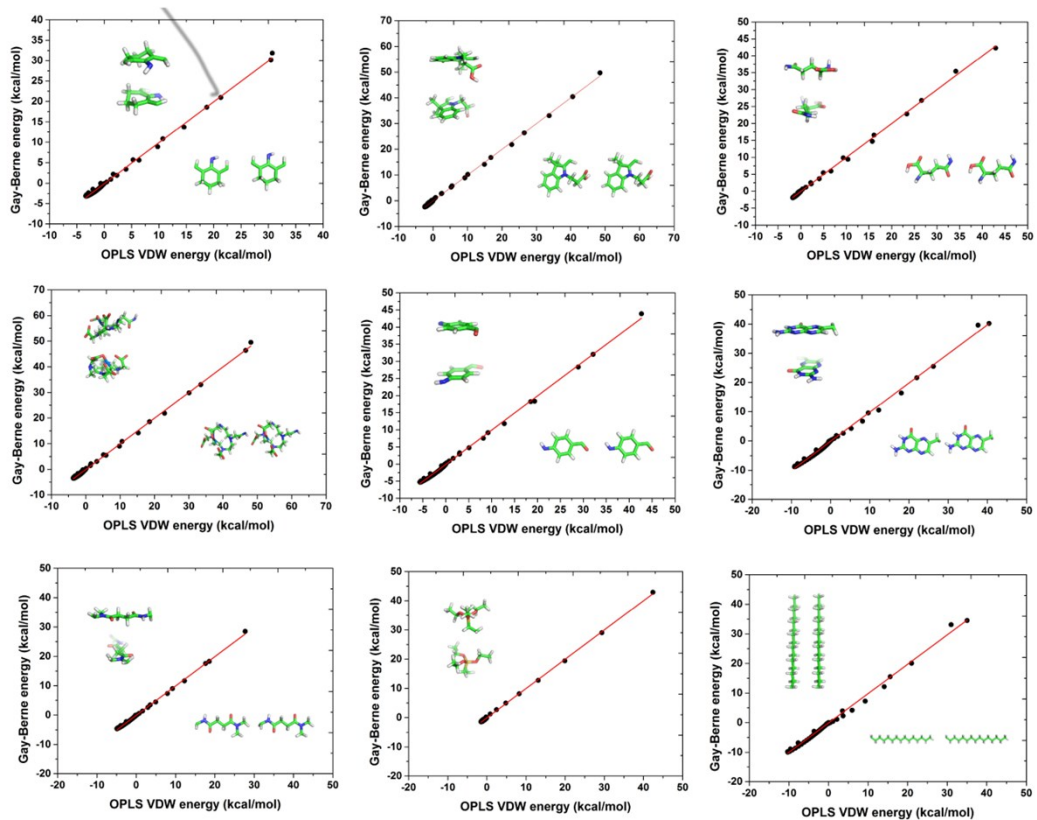


**Figure S9.** Correlations between the GBEMP and atomistic (OPLS) results in the calculations of van der Waals (VDW) interactions between the homodimers respectively. In each figure, insets display the homodimers adopting different orientations.

## GBEMP force field for self-assembly units

```
##### Mu Nu
munudw 2.0 1.0
#####
### Tail rgbtype 11
#####
crslm 11 "Tail1" 211.0 92.0 1070.0 1070.0
gblst 11 112
mplst 11 111
### GB Amide site:Center of Mass
gbers 112 15.171 2.468 0.389 0.067 1.264 10.436
gbsite 112 0.000 0.000 0.000 1.0 0.0 0.0
### EMP site (C)
charge 111 0.000 1.000
mpsite 111 -9.040274 0.394360 -0.008524
#####
### Tail rgbtype 12
#####
crslm 12 "Tail21" 211.0 92.0 1070.0 1070.0
gblst 12 122
mplst 12 121
### GB Amide site:Center of Mass
gbers 122 14.171 2.768 0.389 0.067 1.264 10.436
gbsite 122 0.000 0.000 0.000 1.0 0.0 0.0
### EMP site (C)
charge 121 0.000 1.000
mpsite 121 8.914423 0.046827 0.197846
#####
### Tail rgbtype 13
#####
crslm 13 "Tail22" 211.0 92.0 1070.0 1070.0
gblst 13 132
mplst 13 131
### GB Amide site:Center of Mass
gbers 132 15.171 2.468 0.389 0.067 1.264 10.436
gbsite 132 0.000 0.000 0.000 1.0 0.0 0.0
### EMP site (C)
charge 131 0.000 1.000
mpsite 131 -8.761357 0.417558 -0.365652
#####
### Folic (F21) rgbtype is 21
#####
### Mass Ix IyIz
##
```

```

crslm 21 "F21"    144.0   182.200   785.693  940.864
gblst 21 212
mplst 21 211 213 214
#####
GB C site: Center of mass
gbers 212  6.654   3.128   1.776   0.022   0.826  0.062
gbsite 212  0.000   0.000   0.000   1.0    0.0   0.0
#####
EMP site1
charge 211  0.000   1.315
mpsite 211  3.395736   1.156645   0.083495
#####
EMP site2
charge 213  0.000   1.315
dipole 213 -1.629 -0.249 -0.758
mpsite 213  0.000   0.000   0.000
#####
EMP site3
charge 214  0.000   1.315
mpsite 214 -2.008247 -1.853397   0.007080
#####
### Folic (F22) rgbtype is 22
#####
###          Mass      Ix      lyIz
crslm 22 "F22"    119.000   98.060  488.708  585.853
gblst 22 222
mplst 22 221 223 224
#####
GB site: Center of mass
gbers 222  7.499   2.100   5.600   0.001   1.164  17.260
gbsite 222  0.000   0.000   0.000   1.0    0.0   0.0
#####
EMP site 1
charge 221  0.000   1.315
mpsite 221  2.441284   0.485587   0.095184
#####
EMP site 2
charge 223  0.000   1.315
dipole 223  1.352   0.562 -0.029
mpsite 223  0.000   0.000   0.000
#####
EMP site 3
charge 224  0.000   1.315
mpsite 224 -3.196645 -0.353496 -0.015172
#####
### Folic (F23) rgbtype is 23
#####
###          Mass      Ix      lyIz
crslm 23 "F23"    176.0   307.161  806.362  1111.526
gblst 23 232
mplst 23 231 233
#####
GB site: Center of mass

```

```

gbers  232  7.720   2.068  9.215   0.001   1.214   0.015
gbsite 232  0.000   0.000   0.000    1.0    0.0   0.0
##### EMP site 1
charge 231    0.000   1.315
mpsite 231    3.986443   0.421896   0.001667
##### EMP site 2
charge 233    0.000   1.315
dipole 233    0.991   -0.663    0.009
mpsite 233    0.000   0.000   0.000
#####
### Cy7 (C31) rgbtype is 31
#####
### GB Center of mass
### Ix IyIz
crslm 31 "I31"    99.00  95.000  229.000  270.000
gblst 31 312
mplst 31 311 313
#####
GB Center of mass
gbers 312   6.687   2.800   3.305   0.001   0.913   0.715
gbsite 312   0.000   0.000   0.000    0.0    0.0   1.0
#####
EMP site 1
charge 311    0.000   1.315
mpsite 311    0.246651   2.213083   -0.104018
#####
EMP site 2
charge 313    0.000   1.315
dipole 313    0.021   -0.955    0.249
mpsite 313    0.000   0.000   0.000
#####
### Cy7 (C32) rgbtype is 32
#####
### GB Center of mass
### Ix IyIz
crslm 32 "I32"    99.00  95.000  229.000  270.000
gblst 32 322
mplst 32 321 323
#####
GB Center of mass
gbers 322   6.982   4.050   2.281   3.245   0.702   5.845
gbsite 322   0.000   0.000   0.000    1.0    0.0   0.0
#####
EMP site 1
charge 321    0.000   1.315
mpsite 321    1.078248   2.295007   0.644601
#####
EMP site 2
charge 323    0.000   1.315
dipole 323    0.727   -1.353    0.362
mpsite 323    0.000   0.000   0.000
#####

```

```

### Cy7 (C33) rgbytype is 33
#####
###          Mass      Ix      lyIz
crslm  33 "I33"    99.00  95.000 229.000 270.000
gblst  33 332
mplst  33 331 333
#####
## GB Center of mass
gbers  332   6.982   4.050   2.281   3.245   0.702   5.845
gbsite 332   0.000   0.000   0.000   1.0   0.0   0.0
#####
## EMP site 1
charge 331   0.000   1.315
mpsite 331   0.247227  2.731796  0.333467
#####
## EMP site 2
charge 333   0.000   1.315
dipole 333   -0.505   0.856   -1.112
mpsite 333   0.000   0.000   0.000
#####
### DOSA (D41) rgbytype is 41
#####
###          Mass      Ix      lyIz
crslm  41 "D41"   83.000  68.000 200.000 200.000 Linear
gblst  41 412
mplst  41 411 413
#####
## GB Center of mass
gbers  412   8.421   4.778   3.627   0.774   1.257   2.190
gbsite 412   0.000   0.000   0.000   0.0   0.0   1.0
#####
## EMP site@Center
charge 411   0.000   1.315
mpsite 411   6.816882  1.327703  0.091344
#####
## EMP site@Center
charge 413   0.000   1.315
dipole 413   -1.280  -0.803  -0.685
mpsite 413   0.000   0.000   0.000
#####
### Silipid (S51) rgbytype is 51
#####
###          Mass      Ix      lyIz
crslm  51 "S51"   155.000 154.408 585.922 627.056
gblst  51 512
mplst  51 511 513
#####
## GB Center of mass
gbers  512   7.500   3.426   2.868   0.149   1.057   3.190
gbsite 512   0.000   0.000   0.000   1.0   0.0   0.0
#####
## EMP site@Center

```

```

charge 511 -0.000 1.315
dipole 511 0.039 -0.207 0.278
mpsite 511 1.671428 1.668688 -0.019266
##### EMP site@Center
charge 513 -0.000 1.315
dipole 513 -0.371 0.413 -0.164
mpsite 513 -2.272214 -1.361135 -0.003862
#####
### Silipid (S52) rgbtype is 52
#####
### Mass Ix lyIz
crslm 52 "S52" 191.000 500.0 500.0 500.0 sphere
gblst 52 522
mplst 52 521
#####
### GB Center of mass
gbcrs 522 4.717 4.717 1.427 1.000 1.057 1.000
gbsite 522 0.000 0.000 0.000 0.0 0.0 1.0
#####
### EMP site@Center
charge 521 0.000 1.315
dipole 521 0.268 0.275 -0.526
mpsite 521 0.000 0.000 0.000
#####
##### Bond terms #####
###FOL
crsbond 111 211 250.0 1.480
crsbond 214 221 250.0 1.480
crsbond 224 231 250.0 1.480
###Cy7
crsbond 111 311 250.0 1.480
crsbond 313 321 150.0 3.750
crsbond 313 331 150.0 3.750
##DOA
crsbond 111 411 250.0 1.750
##Silipid
crsbond 131 511 250.0 3.200
crsbond 511 121 250.0 4.400
crsbond 513 521 150.0 7.300
#####
##### Angle terms #####
###FOL
crsangle 112 111 211 100.0 150.0
crsangle 111 211 212 100.0 160.0
crsangle 213 214 221 100.0 130.0
crsangle 214 221 222 100.0 120.0
crsangle 223 224 231 100.0 120.0
crsangle 224 231 232 100.0 120.0

```

```

###Cy7
crsangle 112 111 311 100.0 140.0
crsangle 111 311 312 100.0 120.0
crsangle 311 312 321 100.0 90.0
crsangle 312 321 322 100.0 160.0
crsangle 311 312 331 100.0 80.0
crsangle 312 331 332 100.0 170.0
###DOA
crsangle 112 111 411 100.0 130.0
crsangle 111 411 412 100.0 110.0
##Silipid
crsangle 132 131 511 100.0 160.0
crsangle 131 511 512 100.0 120.0
crsangle 512 513 521 100.0 120.0
crsangle 512 511 121 100.0 70.0
crsangle 511 121 122 100.0 120.0

```

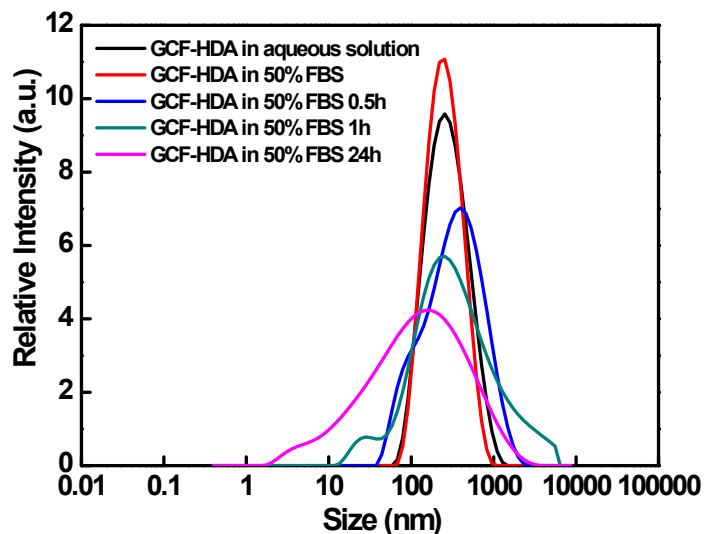


Fig. S10. Stability of liposome NPs in 50% fetal bovine serum (FBS) at different time.

## References

- 1) N. Kamaly, T. Kalber, A. Ahmad, M. H. Oliver, P. W. So, A. H. Herlihy, J. D. Bell, M. R. Jorgensen and A. D. Miller, *Bioconjugate Chem*, 2008, 19, 118-129.
- 2) M. Karplus and J. A. McCammon, *Nat Struct Biol*, 2002, 9, 646-652.

- 3) A. Perez, F. J. Luque and M. Orozco, *Accounts Chem Res*, 2012, **45**, 196-205.
- 4) V. Tozzini, *Curr Opin Struct Biol*, 2005, **15**, 144-150.
- 5) B. A. Merchant and J. D. Madura, *Annu Rep Comput Chem*, 2011, **7**, 67-87.
- 6) H. J. Shen, Z. Xia, G. H. Li and P. Y. Ren, *Annu Rep Comput Chem*, 2012, **8**, 129-148.
- 7) J. G. Gay, *J Chem Phys*, 1981, **74**, 3316-3319.
- 8) D. J. Cleaver, C. M. Care, M. P. Allen and M. P. Neal, *Phys Rev E* 1996, **54**, 559-567.
- 9) B. J. Berne, *J Chem Phys*, 1972, **56**, 4213-4216.
- 10) P. A. Golubkov and P. Ren, *J Chem Phys*, 2006, **125**, 64103-64110.
- 11) P. A. Golubkov, J. C. Wu and P. Ren, *Phys Chem Chem Phys : PCCP*, 2008, **10**, 2050-2057.
- 12) H. Shen, Y. Li, P. Ren, D. Zhang and G. Li, *J Chem Theory Comput*, 2014, **10**, 731-750.